Brazilian Journal
of Chemical
Engineering

ISSN 0104-6632
Printed in Brazil
www.abeq.org.br/bjche

Vol. 36, No. 02, pp. 1061 - 1073, April - June, 2019
dx.doi.org/10.1590/0104-6632.20190362s20180473

ENERGETIC ANALYSIS OF AN ABSORPTION CHILLER USING $NH_3/LiNO_3$ AS AN ALTERNATIVE WORKING FLUID

Alvaro A. S. Lima[1], Alvaro A. V. Ochoa[1,2*], José Â. P. da Costa[1,2], Carlos A. C. dos Santos[3], Márcio V. F. Lima[2] and Frederico D. de Menezes[2]

[1] Universidade Federal de Pernambuco, Programa de Pós-Graduação em Engenharia Mecânica, Recife, PE, Brasil. ORCID: 0000-0003-4224-185X; E-mail: ochoaalvaro@recife.ifpe.edu.br - ORCID: 0000-0001-7597-3358; ORCID: 0000-0001-6599-485X
[2] Instituto Federal de Pernambuco, Recife, PE, Brasil. ORCID: 0000-0003-3559-6564; ORCID: 0000-0003-2186-1849
[3] Universidade Federal da Paraíba, Departamento de Engenharia Mecânica, João Pessoa, PB, Brasil. ORCID: 0000-0002-2840-2787

(Submitted: October 11, 2018 ; Revised: January 17, 2019 ; Accepted: January 22, 2019)

Abstract - This paper presents a thermodynamic model developed for a prototype absorption chiller using $NH_3/LiNO_3$ with 10 kW of nominal capacity. The study was undertaken using thermodynamic modeling based on the mass and energy balance, takes the overall heat transfer coefficients into consideration and uses the characteristic equation method. First, the results obtained from the thermodynamic modeling developed were compared with those obtained from the characteristic equations of thermal power activation and the cooling capacity. These showed good agreement with the experimental data, there being maximum relative errors of around 5% for most of the operational conditions of the system. Secondly, a parametric analysis was made by altering the variables, such as temperature, mass flow rate, and configuring the heat dissipation that influences the overall performance of the prototype chiller.
Keywords: Prototype absorption chiller; Characteristic equation method; Parametric analysis; $NH_3/LiNO_3$.

INTRODUCTION

$LiBr/H_2O$ and NH_3/H_2O, the conventional fluids used in absorption refrigeration systems cause great inconveniences, such as corrosion problems and high pressures, in addition to which there is a need to rectify the solution, which tends to crystallize (Akrami et al., 2018; Guido et al., 2018). The binary pair, lithium nitrate/ammonia binary, has been used as an alternative solution for these systems (Libotean et al., 2007 and 2008; Cuenca et al., 2014). The mixture ($NH_3/LiNO_3$) has shown good results when compared to the mixtures used in commercial systems ($LiBr/H_2O$ and also NH_3/H_2O), especially when solar energy is used as an activation source of the system (Amaris et al., 2014; Buonomano et al., 2018).

Several studies on absorption systems that use $NH_3/LiNO_3$ have been conducted, some of which seek to take experimental approaches (Moreno-Quintanar et al., 2011 and 2012; Jimenez and Rivera, 2014; Cai et al., 2016; Jiang et al., 2017) while others take theoretical approaches (Acuña et al., 2013; Farshi et al., 2014; Alvarez et al., 2016; Azhar and Siddiqui, 2017; Maryami and Dehghan, 2017; Sabbagh and Gómez, 2018), especially in the direction of creating prototypes. This is seen in the literature (Hernández-Magallanes et al., 2014; Zamora et al., 2014 and 2015). Moreno-Quintanar et al. (2012) made a comparison with a solar-powered intermittent absorption refrigeration system, which takes both a binary mixture ($NH_3/LiNO_3$) and also a ternary mixture ($NH_3/LiNO_3+H_2O$) into account, their goal being to verify the best mixture for the solar absorption chiller. They found that the advantages offered by the ternary mixture were greater than those presented by the binary mixture ($NH_3/LiNO_3$). Studies by Zamora et al. (2014, 2015) developed two

* Corresponding author: Alvaro A. O. Villa - E-mail: ochoaalvaro@recife.ifpe.edu.br

pre-industrial absorption chillers, one with a water-cooled system and the other with an air-cooled system, which were built with brazed plate heat exchangers. The goals of these papers were to optimize the chiller, the focus being on the circulation pump, and also to characterize these pre-industrial chillers at part-load.

To compare configurations of absorption refrigeration systems and their performance, Domínguez-Inzunza et al. (2014) compared five configurations of operational absorption systems (namely, those of half-effect; single-effect; double-effect in series; double-inverse and triple-effect) using ammonia/lithium nitrate solution as the working pair. The results showed that the single-effect chiller has the simplest configuration in comparison to the other chillers analyzed and also its Coefficient of Performance (COP) is almost twice as high as those obtained with the half-effect cycle. In their paper, Cai et al. (2015) introduced a new component to improve the thermal performance of a novel air-cooled double effect absorption refrigeration system that could use ammonia/lithium nitrate and ammonia/sodium thiocyanate solutions as working fluids and a high temperature source to activate the cycle. In the same context, although using a two-stage configuration of a thermodynamic double-effect absorption cycle with ammonia/lithium nitrate, Ventas et al. (2016) found that the maximum COP could reach 1.25 when the driven temperature was around 100°C. Cai et al. (2016) conducted an experimental study of an air-cooled type single-effect absorption refrigeration cycle that uses two different solutions ($NH_3/LiNO_3$ and ammonia-sodium thiocyanate) as working pairs, with a view to determining how these influenced the evaporation temperature and capacity of the chiller. Ventas et al. (2017) conducted a study with a view to proposing a $NH_3/LiNO_3$ two-stage double-effect absorption chiller for cogeneration systems that produce electricity and cooling using solar thermal or residual heat as energy sources. It was found that a combined power and cooling system allows the production of power to be adapted either to the demand for cooling or to the demand for power by splitting the vapor generated.

On using this alternative mixture ($NH_3/LiNO_3$) in absorption systems, some advantages were demonstrated, mainly with respect to the simplicity of the configuration of the cycle, due to excluding the rectifier in absorption systems that use ammonia/water as the working fluid. From this context, numerous experimental proposals were put forward for different applications of these systems, such as thermal comfort and also refrigeration (Domínguez-Inzunza et al., 2014; Hernández-Magallanes et al., 2014; Jiménez and Rivera, 2014; Zamora et al., 2014 and 2015; Cai et al., 2016).

In this paper, a complete energetic analysis of the prototype absorption chiller is presented. The study uses thermodynamic modeling based on the mass and energy balances that take the overall heat transfer coefficients into consideration. Its uses the characteristic equation method by applying the Duhring rule of the internal temperature based on the saturation mean temperatures and the Duhring slope. It also conducts a sensitivity analysis of the parameters such as the temperatures of hot, cold and chilled water and the mass flow rates, the configuration of the heat dissipation systems (series and parallel) and also the effect of the overheating introduced at the outlet of the evaporator. The goal is to increase the thermal COP of the prototype chiller.

METHODOLOGY

The absorption refrigeration equipment modeled in this paper is a 10 kW single-effect hot water-fired absorption chiller of nominal capacity which uses $NH_3/LiNO_3$ as the working fluid. It was designed, built and tested by the SOLAFRIO and CONFISOL project (Zamora, 2012). This prototype was modeled in the steady state, based on the mass, species and energy balances. As is known, a single-effect absorption refrigeration system is a device that, basically, consists of a generator, a condenser, an absorber, an evaporator, expansion valves, a solution heat exchanger and pumps, see Figure 1. However, this model includes a refrigerant heat exchanger in order to enhance the efficiency of the absorption system.

In addition to the generator, condenser, absorber, evaporator, there are two plate heat exchangers: one for the solution and another for the refrigerant. These components were chosen because of their compactness. The operation takes place using three internal and external fluids. The internal ones are divided into the $NH_3/LiNO_3$ solution, which passes through points 1 - 6 (which are responsible for the desorption and absorption processes), and the refrigerant vapor, which passes through points 7-10, and points 19 and 20 (which is responsible for the cooling effect).

The external circuits are divided into three, namely, the hot, cold and chilled water circuits. The hot water circuit (points 11-12) represents the activation source for the absorption chiller, while the cold water circuit (points 13-16) represents the dissipation source of the systems, and the chilled water circuit (points 17-18) represents the cooling capacity of the chiller.

Thermodynamic Modeling of the prototype absorption chiller

In the thermodynamic modeling of the prototype, see Figure 1, the external circuits (cold, hot and chilled water) and their interactions with the internal circuit (solution and/or refrigerant) had to be included. This was achieved by using the characteristic equations of each heat exchanger. The equation that characterizes

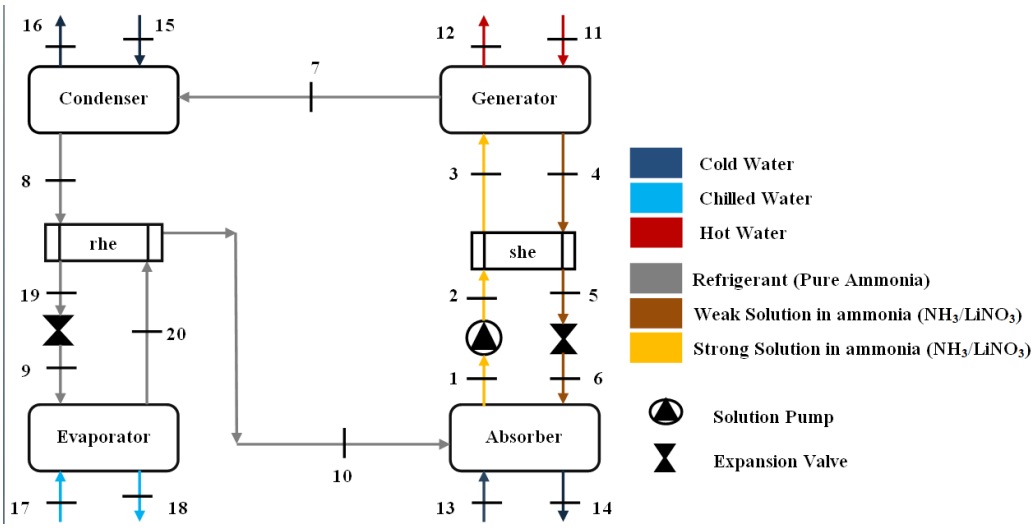

Figure 1. Diagram of the Prototype Absorption Chiller.

the heat exchanger is based on the product (UA) and the logarithmic average temperature (ΔT_{ln}), the latter being the boundary condition between the internal circuit and the external fluid. This modeling of the internal circuit with external circuits allows the output conditions (pressures, temperatures, energy flows) of the chiller to be checked based on the variations made to the system (thermal load, source activation, cooling circuit). To construct the thermodynamic model of the prototype, the following simplifying assumptions were considered:

- The system is in steady state;
- The temperature, pressure and concentration are homogeneous in each component;
- The refrigerant circuit consists exclusively of pure ammonia;
- There are only two pressure levels, high (generator - condenser) and low (absorber - evaporator);
- A variation in pressure occurs only in the expansion valves;
- The rich solution leaving the absorber is in saturation conditions at the pressure and temperature of the absorber;
- The heat exchange with the neighborhood is negligible;
- The expansion valves are considered adiabatic.

The properties of the working fluids of the system were determined from the correlations found in the literature. For pure ammonia, the correlations presented by Tillner-Roth et al. (1993) were used and for the $NH_3/LiNO_3$ solution, the vapor pressure specific heat, density, viscosity and enthalpy were determined by using, the correlations found by the CREVER group (Libotean et al., 2007 and 2008; Cuenca et al., 2014).

Table 1 shows the equations of the mass, species and energy balances for all the components of the absorption chiller and it also shows the set of equations of the external circuitry and the heat transfer equations of the heat exchangers. These equations represent the overall energetic modeling of the prototype as can be seen in Ochoa et al. (2014a and 2014b; Ochoa et al., 2016; Ochoa et al., 2017).

The subscript X represents the components (absorber, evaporator, condenser and generator) of the chiller. The temperature of the external water circuit is represented by the letter (t) and the temperatures of the internal circuit of the chiller are represented by the letter (T).

Characteristic Equation Method

Based on the information found in the open literature, specifically in Albers and Ziegler (2015) and Zinet et al. (2012), the characteristic equation method is based on the thermodynamic fundamentals and nominal characteristics of the chiller. The aim is to determine the behavior of the absorption chiller considering the average temperatures of the cold,

Table 1. Mass, species and energy balances, and heat transfer equations of the heat exchangers modeled.

Mass Balance	Species Balance	Energy Balance
$\sum_{in} \dot{m} = \sum_{out} \dot{m}$	$\sum_{in} \dot{m}X_x = \sum_{out} \dot{m}X_y$	$\dot{E}_{in} = \dot{E}_{out}$
External Circuit – Heat Transfer Equations – of the Heat Exchangers		
$\dot{Q}_x = \dot{m}_{sol}(h_{in} - h_{out})$	$\dot{Q}_X = UA_X \Delta Tlm_X$	$\Delta Tlm_X = \frac{(t_{X,in} - T_{X,in}) - (t_{X,out} - T_{X,out})}{Ln\left\{\frac{(t_{X,in} - T_{X,in})}{(t_{X,out} - T_{X,out})}\right\}}$

hot and chilled water (external circuits) and specific characteristics of the chiller, such as the overall heat transfer coefficients and flow rates. Implementation takes the Duhring rule into account, thus allowing both the internal average temperatures of each heat exchanger of the chiller to be identified and the weak and strong concentrations (X_{sol}) of the system and the temperatures of the saturated solution ($T_{sat,sol}$) from a linear equation with slope B and intersection Z, expressed as:

$$T_{sat,sol} = B(X_{sol}) \cdot T_{sat,ref} + Z \cdot (X_{sol}) \quad (1)$$

This considers the four main heat exchangers (Absorber, Evaporator, Condenser and Generator), and lets calculations be made of the heat flow ($\dot{Q}i$), based on the overall heat transfer coefficient and the area of the heat exchanger, the product (UA_X), and the average logarithmic difference (ΔTlm_X) as shown in Table 1. To simplify the equations and according to the literature for heat exchangers, the analysis of absorption refrigeration systems (Kohlenbach and Ziegler, 2008 and 2008b; Myat et al., 2011; Ochoa et al., 2016 and 2017) and the term (ΔTlm) of the characteristic equation can be replaced by the mean difference in temperature between the hot and cold fluids ($\Delta Tlm_X \approx |t_X - T_X|$). Where t_X is the average temperature of the external fluid and T_X is the average temperature of the internal fluid of the flows of the heat exchanger.

The characteristic equation method was described by applying the First Law of Thermodynamics to the absorption refrigeration system, taking into account a steady-state regime with the energy and mass balances of the system. Table 2 shows the equations of the first part of implementing the characteristic equation method of the prototype chiller.

By applying the Duhring rule for two temperature levels, Eq. 1, (high and low), the relationships found were:

$$T_G - T_A = B(X_{sol}) \cdot (T_C - T_E) \quad (2)$$

The B term of equation 2 represents the slope of the Duhring diagram. By combining the equations from Table 2 and equation (2), the average external temperatures of the cold, hot and chilled water circuits are determined, expressed as:

$$\begin{aligned} t_G - t_A - B \cdot (t_C - t_E) &= \dot{Q}_E \cdot \left(\frac{G}{UA_G} + \frac{A}{UA_A} \right) + \dot{Q}_{loss} \cdot \\ &\cdot \left(\frac{1}{UA_G} + \frac{1}{UA_A} \right) + B \cdot \dot{Q}_E \cdot \left(\frac{C}{UA_C} + \frac{1}{UA_E} \right) \end{aligned} \quad (3)$$

The term on the left can be represented by the total temperature difference ($\Delta\Delta t$), as:

$$\Delta\Delta t = t_G - t_A - B \cdot (t_C - t_E) = \Delta t_{thrust} - B \cdot \Delta t_{lift} \quad (4)$$

Eq. 4 could be interpreted as the difference between the temperature thrust $\Delta t_{thrust} = (t_G - t_A)$ and the temperature lift $\Delta t_{lift} = (t_C - t_E)$. The total temperature difference can also be defined in terms of the design parameters, such as:

$$\Delta\Delta t = \frac{\dot{Q}_E + \dfrac{\dot{Q}_{loss} \cdot \left(\dfrac{1}{UA_G} + \dfrac{1}{UA_A} \right)}{\left[\dfrac{G}{UA_G} + \dfrac{A}{UA_A} + B \cdot \left(\dfrac{C}{UA_C} + \dfrac{1}{UA_E} \right) \right]}}{\dfrac{1}{\left[\dfrac{G}{UA_G} + \dfrac{A}{UA_A} + B \cdot \left(\dfrac{C}{UA_C} + \dfrac{1}{UA_E} \right) \right]}} \quad (5)$$

This fraction of the total temperature difference can be simplified based on two parameters: (S_E) representing the proportion of the global coefficient of each component of the chiller Eq. (6); and (α_E), which represents the distribution of the overall heat transfer coefficients inside the equipment Eq. (7), such as:

$$S_E = \frac{1}{\left[\dfrac{G}{UA_G} + \dfrac{A}{UA_A} + B \cdot \left(\dfrac{C}{UA_C} + \dfrac{1}{UA_E} \right) \right]} \quad (6)$$

$$\alpha_E = \frac{\left(\dfrac{1}{UA_G} + \dfrac{1}{UA_A} \right)}{\left[\dfrac{G}{UA_G} + \dfrac{A}{UA_A} + B \cdot \left(\dfrac{C}{UA_C} + \dfrac{1}{UA_E} \right) \right]} \quad (7)$$

Table 2. First Part of the Equation characteristic Method of the absorption chiller.

Generator	Absorber	Evaporator	Condenser
$\dot{Q}_G = G \cdot \dot{Q}_E + \dot{Q}_{loss}$	$\dot{Q}_A = A \cdot \dot{Q}_E + \dot{Q}_{loss}$	$\dot{Q}_E$	$\dot{Q}_C = C \cdot \dot{Q}_E$
Solution and Refrigerant Heat exchangers			
$\dot{Q}_{loss} = \dot{Q}_{max} - \dot{Q}_{she}$	$\dot{Q}_{max} = \dot{m}_{weak}(h_4 - h_1)$	$C = C' \cdot R$	
Generator - Absorber		**Evaporator - Condenser**	
$G \cdot \dot{Q}_E + \dot{Q}_{loss} = UA_G(t_G - T_G)$		$\dot{Q}_E = UA_E(t_E - T_E)$	
$A \cdot \dot{Q}_E + \dot{Q}_{loss} = UA_A(T_A - t_A)$		$C \cdot \dot{Q}_E = UA_C(T_C - t_c)$	
$A = \frac{(h_{10} - h_4)}{(h_{10} - h_8)}$	$G = \frac{(h_7 - h_4)}{(h_{10} - h_8)}$	$R = \frac{(h_{10} - h_{20})}{(h_{20} - h_{19})}$	$C' = \frac{(h_7 - h_8)}{(h_8 - h_{19})}$

The total temperature difference could be defined as Equation 8:

$$\Delta\Delta t = \frac{\dot{Q}_E}{S_E} + \Delta\Delta t_{min\,E} \tag{8}$$

The minimum total temperature difference ($\Delta\Delta t_{minE}$) represents a relationship between the parameters (S_E, α_E and $\dot{Q}_{loss}$), expressed as:

$$\Delta\Delta t_{min\,E} = \frac{\alpha_E \cdot \dot{Q}_{loss}}{S_E} \tag{9}$$

The thermal power activation (generator) and cooling capacity (evaporator) of the absorption chiller can be expressed as:

$$\dot{Q}_E = S_E \cdot \left(\Delta\Delta t - \Delta\Delta t_{min\,E}\right) \tag{10}$$

$$\dot{Q}_G = G \cdot \left[S_E \cdot \left(\Delta\Delta t - \Delta\Delta t_{min\,E}\right)\right] + \frac{S_E}{\alpha_E} \cdot \Delta\Delta t_{min\,E} \tag{11}$$

The full modeling and implementation of the characteristic equation method of the prototype chiller are detailed in Ochoa et al. (2017).

Coefficient of Performance of the Chiller (COP)

The COP of the chiller can be expressed as:

$$COP = \frac{\dot{Q}_E}{\dot{Q}_G} = \frac{S_E \cdot \left(\Delta\Delta t - \Delta\Delta t_{min\,E}\right)}{G \cdot \left[S_E \cdot \left(\Delta\Delta t - \Delta\Delta t_{min\,E}\right)\right] + \dot{Q}_{loss}} = \frac{\Delta\Delta t - \Delta\Delta t_{min\,E}}{G \cdot \Delta\Delta t \cdot \left(S_E \cdot \left(\frac{1}{\alpha_E} - G\right)\right) + \Delta\Delta t_{min\,E}} \tag{12}$$

DISCUSSION AND RESULTS

The energetic analysis using the theoretical thermodynamic modeling based on the mass, species and energy balances and the characteristic equation method was compared with experimental data collected from the paper by Zamora (2012) and also by adapting the thermal power activation and cooling capacity based on two correlations in accordance with the method found in the literature (Puig et al., 2010). In the second part, a parametric analysis was conducted to verify the influence of the operational parameters on the performance of the prototype chiller.

Nominal Conditions of the Prototype $NH_3/LiNO_3$ Absorption Chiller

The nominal temperature conditions of the cold, chilled and hot water of the prototype are shown in Table 3 (Zamora, 2012). The Products (*UA*) were estimated from the nominal conditions used in the equation:

$$UA = \frac{\dot{Q}}{\Delta Tlm} \tag{13}$$

Comparison of the experimental data and numerical results of the thermodynamic modeling

To validate the thermodynamic modeling applied for the prototype absorption chiller, 10 operational scenarios were selected that take the flows of hot, cold and chilled water into account. The experimental data and the numerical results obtained were compared, considering the (hot, cold and chilled) outlet water streams. Figures 2 and 3 show the temperature profiles of the hot and chilled water, respectively, that were simulated by the model and those determined experimentally by Zamora (2012).

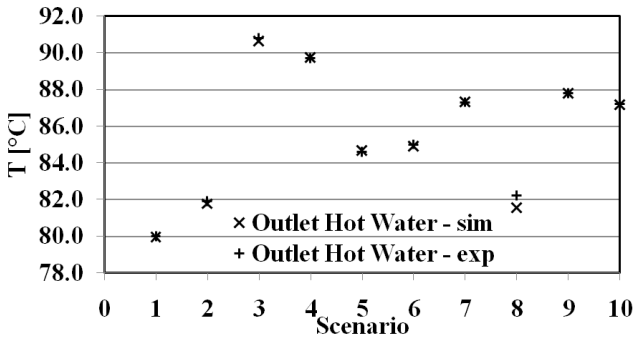

Figure 2. Comparison of the temperature profiles obtained by the thermodynamic modeling and the experimental data for the Hot water.

Table 3. Nominal Conditions of the Prototype Absorption Chiller.

Mass flows (kg.s^{-1})		Temperatures (°C)	
Hot water	0.8330	Inlet Hot water	90.0
Cold Water	0.8000	Inlet Cold water - Absorber	37.5
Chilled Water	0.7986	Inlet Cold water - Condenser	37.5
Rich Solution ($NH_3/LiNO_3$)	0.1000	Outlet Chilled Water	15.0
UA Product (kW K^{-1})			
Generator	3.69	Evaporator	1.56
Condenser	2.43	SHE	1.06
Absorber	3.00	RHE	0.05
Pump Efficiency (%)		100	

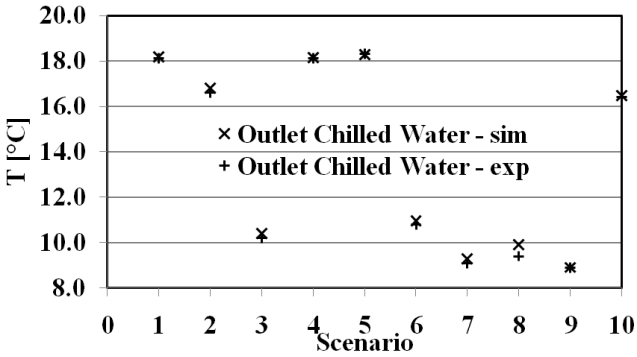

Figure 3. Comparison of the temperature profiles obtained by the thermodynamic modeling and the experimental data for the Chilled water.

For the hot water circuit, the values obtained by the thermodynamic modeling and from experimental data showed the same trend, there being a minimal divergence between them. In the case of the chilled water circuit, the comparison showed a similar result to that of the hot water circuit; namely the same trend was followed and there was also a slight divergence between the simulated and experimental values. The minimum and maximum errors are 0.02% and 6% for the chilled water and the hot water, respectively. Therefore, the adjustment between the numerical and the experimental data can be considered good and, hence, the comparison is very good. As to the cold water circuit, the behavior is the same as that shown in the case of the hot water, but there is a little more divergence between the numerical and experimental data in all 10 of the scenarios. This fact can be attributed to the uncertainties of the experimental data (around 5%, as found by Zamora, 2012).

Comparison of the experimental data with the results from the characteristic equation

To validate the results obtained by implementing the characteristic equation method, a comparison with the experimental data was made in two ways: First, the results between the real experimental data were compared and secondly, so were the results from the experimental correlation coming from the adjustment of the experimental data, based on the data used in Puig et al. (2010).

The adjusted experimental correlations obtained from the data presented in Zamora (2012) and adapted by the methodology presented in Puig et al. (2010) can be expressed as:

$$\dot{Q}_{e\_exp\_corr} = a_e \cdot T_{ch} - b_e \cdot T_{ac} + c_e \cdot T_g + d_e \quad (14)$$

$$\dot{Q}_{g\_exp\_corr} = a_g \cdot T_{ch} - b_g \cdot T_{ac} + c_g \cdot T_g + d_g \quad (15)$$

The experimental data of the Prototype Absorption chiller were extracted from the study by Zamora (2012) considering the following operational temperature ranges: 7-15°C chilled water, 80-100°C hot water, and 32-45°C cold water. Seventeen (17) operating conditions of the absorption chiller were selected. Table 4 shows the values of the parameters of equations 16 and 17.

Figures 4 and 5 compare the results of using the thermal activation power and the cooling capacity of the prototype, respectively. These were obtained by the characteristic equation method ($\dot{Q}_{g\_ce}$; $\dot{Q}_{e\_ce}$), experimental data ($\dot{Q}_{g\_exp}$; $\dot{Q}_{e\_exp}$) and the adjusted experimental correlations ($\dot{Q}_{g\_corr}$; $\dot{Q}_{e\_corr}$), arising from the total difference in temperature that considered the whole operational range of the equipment.

Figures 6 and 7 show that results obtained by implementing the characteristic equation method for

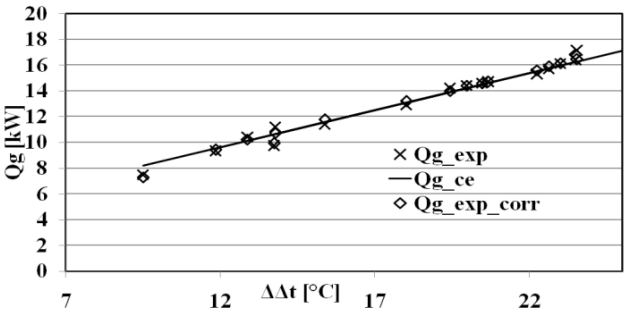

Figure 4. Comparison of the results obtained by the characteristic equation method, real experimental data and the correlations adjusted for the Thermal activation power ($\dot{Q}_g$).

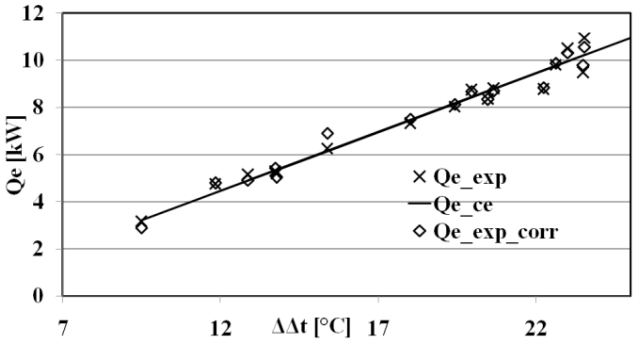

Figure 5. Comparison of the results obtained by the characteristic equation method, real experimental data and the correlations adjusted for the Cooling capacity ($\dot{Q}_e$).

Table 4. Coefficients Values of equations 16 and 17.

Parameter [kW]	a (kW.K^{-1})	b (kW.K^{-1})	c (kW.K^{-1})	d (kW)
$\dot{Q}_{e\_exp\_corr}$	0,50449	0,7957	0,32577	2,91347
$\dot{Q}_{g\_exp\_corr}$	0,55344	1,0164	0,48662	2,05125

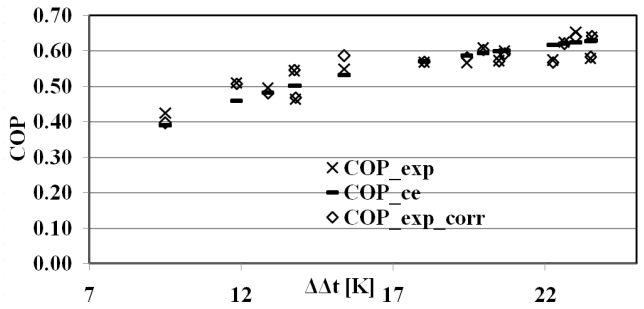

Figure 6. Comparison of the results obtained by the characteristic equation method, real experimental data and the adjusted correlations for the COP.

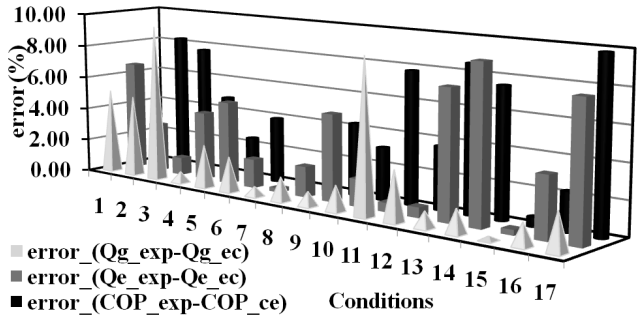

Figure 7. Comparison of the results obtained by the characteristic equation method, real experimental data and the adjusted correlations taking into the account the Minimum and Maximum errors.

the thermal activation power and the cooling capacity fit well over the operating range of the absorption chiller. This was considered a good adjustment since the minimum and maximum errors were around 1 to 10%, which is good when the complexity of the absorption and desorption processes in the cycle are considered, and also, because of the assumptions that were made to simulate the prototype chiller.

Figure 6 shows the comparison of the COP of the absorption chiller results obtained by the characteristic equation method (COP_{ce}), the experimental data (COP_{exp}) and the adjusted experimental correlation (COP_{exp_corr}), arising from the total difference in temperature that considered the whole operational range of the equipment. Figure 7 shows their minimum and maximum errors.

Note that there are differences between results of the COP, see Figure 6, that could be due to propagation of error in the thermal activation power and cooling capacity. Once more, these were attributed to uncertainties in the experimental data (around 5%) and also to simplifying assumptions of the modeling.

Despite these errors, the adjustment can be considered good because, for most operating conditions, these deviations were not greater than 5%, especially at the nominal operational conditions of the prototype, namely when the hot, chilled and cold water were at temperatures of 90°C, 15°C and 37.5°C, respectively, represented by a $\Delta\Delta t$ of 23K where the deviation was lower than 1%.

As already mentioned, Figure 7 shows good agreement between the results obtained from the characteristic equation and the experimental data, and also when the experimental data and the results from the adjusted correlation are compared. For most of the operational range of the chiller, including the nominal condition, the deviations were 5% lower. The maximum errors of the results were found in the thermal power activation, around 9%, as was the minimum error of around 0.2%. These errors lead to maximum and minimum errors in the COP of 10% and 0.6%, respectively. Therefore, in order to tackle the overall uncertainties involved in operating the prototype, this could be considered a good adjustment for predicting the behavior of the systems.

Parametric analysis of the prototype $NH_3/LiNO_3$ absorption refrigeration chiller.

The idea of this parametric analysis was to verify the thermodynamics of the different technical parameters such as: the type of configuration of series and parallel heat dissipation circuit and the temperatures of the (hot, cold and chilled water) external circuits, the mass flow rate of the ammonia-rich solution in the internal circuit of the prototype chiller, the influence of the flow mass rate according to the dissipation system and finally, the influence of the overheating at the outlet of the evaporator. In the parametric analysis, the effects were compared including and excluding the heat exchanger of the refrigerant of the prototype chiller.

COP Profile based on the configuration of the heat dissipation circuit (series and parallel) and the temperatures of the hot, cold and chilled water

Single-effect absorption systems can basically use two dissipation circuit configurations; series or parallel. The series configuration predicts that a single water line will flow through the absorber - condenser assembly, i.e., the circulation water passes first through the absorber and later either through the condenser or the dissipation system (cooling tower, air heater, air dissipation). On the other hand, the parallel configuration predicts that the line coming from the dissipation system will be divided into two sub lines, which keep the same inlet temperature, i.e., the cold dissipation water will enter the absorber and the condenser at the same temperature. These settings have different behaviors with regard to the performance of the chiller. In this section, it was decided to vary the COP based on the configuration with the system, whether or not the refrigerant heat exchanger was used, but nevertheless taking the hot and cold water inlet temperatures and the chilled water outlet into account.

In the parallel configuration the flow is divided into two streams that keep the same value for the water flow rate. This is done with the intention of having the same cold water inlet temperature in the two heat exchangers that integrate the heat dissipation system.

Figures 8 to 10 show the COP profile based on the inlet temperatures of the hot and cold water and the output of the chilled water, respectively.

Initially, it should be noted that the behavior in terms of magnitudes is the same as in other simulations, i.e., the inclusion of the refrigerant heat exchanger increases the COP by approximately 3%.

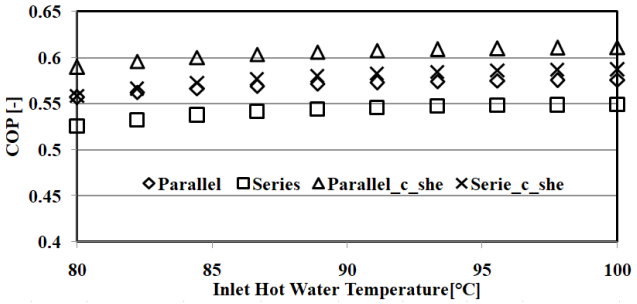

Figure 8. COP Profile (with and without a refrigerant heat exchanger) varying the inlet hot water temperature considering the series and parallel configuration of the heat dissipation system.

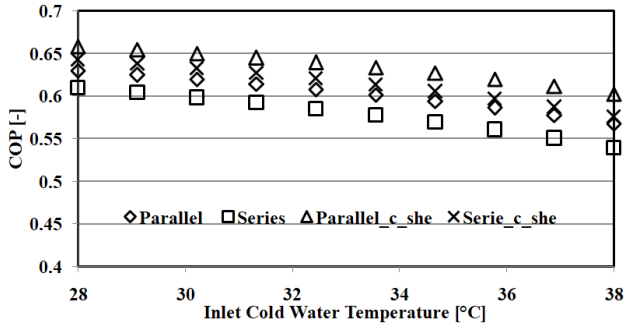

Figure 9. COP Profile (with and without refrigerant heat exchanger) varying the inlet cold water temperature considering the series and parallel configuration of the heat dissipation system.

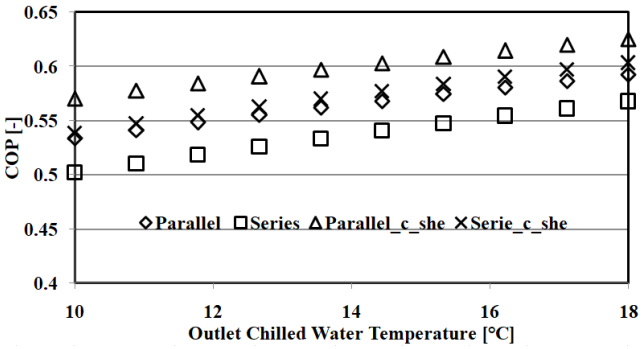

Figure 10. COP Profile (with and without refrigerant heat exchanger) varying the inlet temperature of the inlet chilled water, considering the series and parallel configuration of the heat dissipation system.

Note that the parallel configuration results in the chiller performing better when the cold water dissipation flow is the same in both cases, since this configuration guarantees the same capacity to dissipate heat in both components (absorber and condenser). This is because the performance of the absorption cycle is better when there is a parallel configuration of the heat dissipation circuit because the temperature of the inlet water that goes to the condenser and the absorber is the same, and also the mass flow rate has the same value. Thus, this gives the system more capacity to dissipate heat, i.e., the useful dissipation temperature is low and the total flow rate of the cooling water is high. As to the series configuration, the values of the inlet water temperature are different. This is because the water first flows into the absorber and after the heat in this component is dissipated, the water passes through the condenser but at a higher temperature than at its inlet. Therefore, the capacity of the condenser is lower than in the absorption cycle with the parallel heat dissipation configuration (absorber - condenser). This has been discussed in the literature (Domínguez-Inzunza et al., 2014; Herold et al., 2016; Chahartaghi et al., 2019).

Comparisons of the series and parallel configurations when analyzing the chiller with and without the refrigerant heat exchanger showed there was a maximum percentage increase of 5% when the temperature of the chilled water was varied and a minimum increase of 4% of the COP when the temperature of the cold water is varied.

COP Profile based on the mass flow rate of the ammonia-rich solution considering the dissipation temperature (cold water) and the chilled water temperature

This section shows the influence of the increase in the mass flow rate of the solution on the COP, but considering the dissipation temperatures (in the range of 28-38°C) and chilled water temperatures (in the range of range 2-10°C) of the prototype chiller, see Figures 11-12.

Figures 11 and 12 show the influence of the temperatures of the dissipated water and the chilled water, considering the prototype absorption refrigeration system without the refrigerant heat exchanger.

Figures 13 and 14 show the influence of the temperatures of the dissipated water and the chilled water temperatures considering the prototype absorption refrigeration system with the refrigerant heat exchanger.

In general, Figures 13 and 14 show that the behavior is maintained due to including the refrigerant heat exchanger, which always provides higher COPs than the prototype without this heat exchanger, at the same operating conditions. This is because the prototype

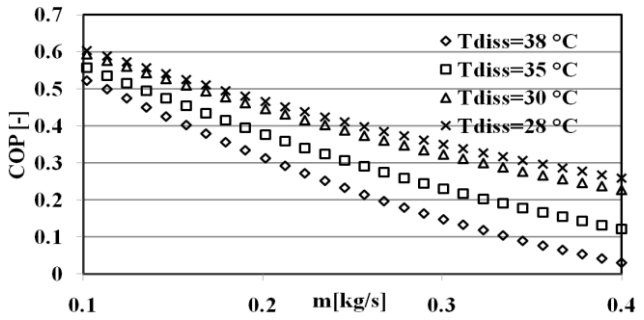

Figure 11. COP Profile (without rhe) varying the ammonia rich mass flow rate for dissipation water and chilled water temperatures at nominal conditions.

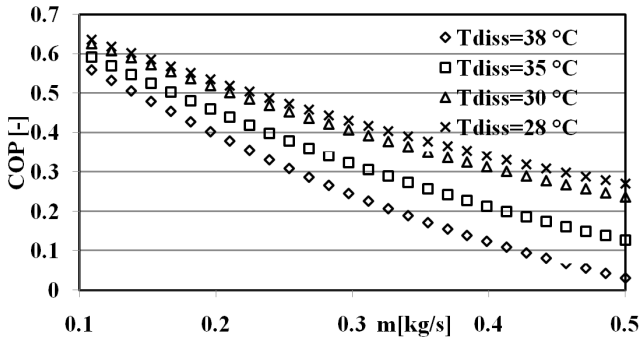

Figure 12. COP Profile (without rhe) varying the ammonia rich mass flow rate for dissipation water and chilled water temperatures at different conditions.

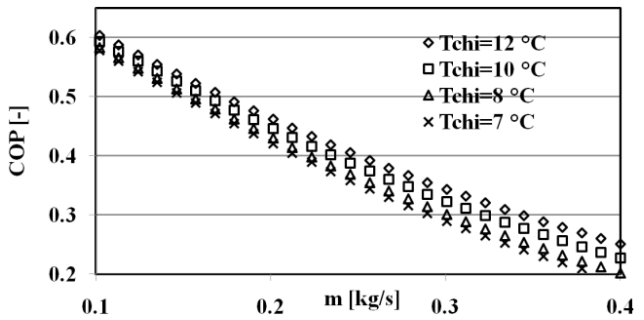

Figure 13. COP Profile (with rhe) varying the ammonia rich mass flow rate for dissipation water and chilled water temperatures at nominal conditions.

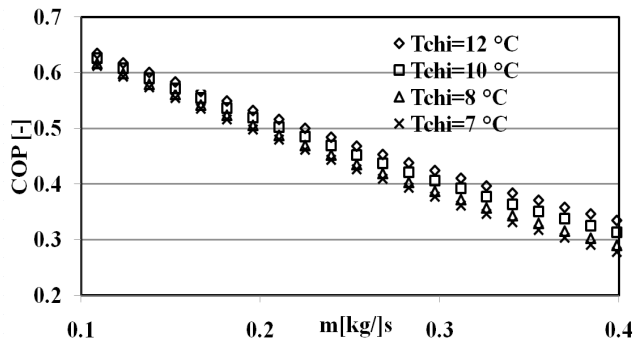

Figure 14. COP Profile (with rhe) varying the ammonia rich mass flow rate for dissipation water and chilled water temperatures at different conditions.

needs to generate more refrigerant vapor, i.e., a higher activation power is required (generator heat flow), but the heat removal rate decreases (Evaporator heat flow) due to the low temperatures of the chilled water and, therefore, there is a higher heat rate of dissipation in the prototype.

It is important to note that, on varying the temperature of the chilled water (cooling effect), its return is smaller, which directly affects the cooling capacity of the prototype, whenever the system design conditions are used.

COP profile based on the overheating at the outlet of the evaporator.

This section shows the influence of overheating at the evaporator outlet on generating vapor and hence on the COP of the prototype considering a fixed flow of the ammonia-rich solution required by the solution pump and varying the inlet hot water temperature. In addition to analyzing the effect of overheating under the nominal conditions.

Figure 15 shows the difference between the COP and the mass flow of the vapor produced in the generator (desorption process) of the chiller with and without overheating at the evaporator outlet based on the temperature of the hot water inlet, while Figure 16 shows this difference under nominal conditions.

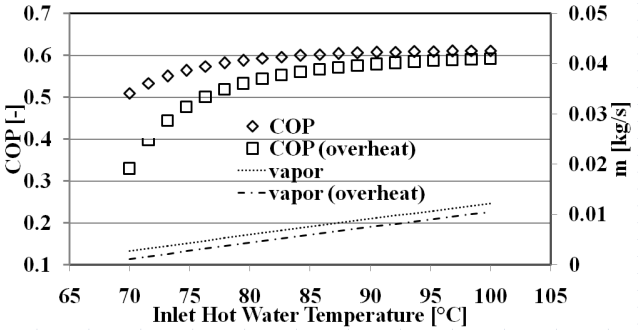

Figure 15. Comparison of the COP and vapor mass flow rate considering (with/without) overheating at the evaporator output varying the inlet hot water temperature, including the refrigerant heat exchanger

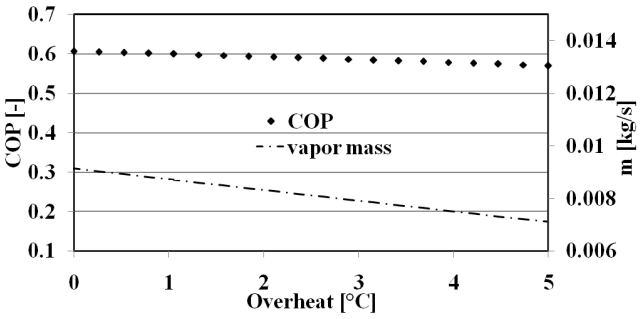

Figure 16. Comparison of the COP and vapor mass flow rate considering (with/without) overheating at the evaporator output varying the overheating, considering nominal conditions.

The effect of overheating at the outlet of the evaporator can be favorable in operational terms, since in energy terms this reduces the COP of the system compared to the COP of the chiller without this overheating. This effect can be understood by producing the refrigerant vapor of the generator (ammonia desorption process), since when the system overheats, it tends to produce less refrigerant vapor and, therefore, the refrigerating capacity in the evaporator is also reduced, leading to smaller COPs. This decrease is more relevant at low temperatures of the hot water (70-80°C) where the difference may be 18%, but at temperatures higher than 80°C, this is reduced by up to 3%. This fact can be attributed to vapor being generated, since the lower temperatures of the hot water will lead to refrigerant vapor being generated in both cases; however, whenever there is overheating, the rate at which refrigerant vapor is generated is even smaller.

Figure 16 shows the progressive degrading effect of COP on the chiller when overheating is introduced at the evaporator outlet, so that the generation of refrigerant vapor has a negative rate of production, leading to a lower capacity to remove the thermal heat from the evaporator and therefore reducing the COP of the system. This is proportional to the increase in this overheating at the evaporator outlet. In quantitative terms, the COP was reduced by approximately 6% since the overheating began to be added (0 to 5°C).

CONCLUSIONS

Implementing the thermodynamic modeling and the characteristic equation method enabled the behavior of the prototype absorption chiller to be determined with good accuracy. This was proven because the results obtained after comparing them were good for most of the operational range. In this paper, the parametric analysis of the prototype was presented. In summary, the most significant results of this study are as follows:

- Comparison of the results of thermal power activation and the cooling capacity of the prototype absorption chiller, obtained by theoretical modeling and the characteristic equation values was very good, since the errors found were lower by 5% for most of the range of operational conditions;
- The thermodynamic modeling and the characteristic equation method led to being able to determine the behavior of the prototype with good accuracy for all operational conditions;
- The effect of considering the configuration of the heat dissipation system (cold water) was slightly higher when the system operates in parallel rather than in series;
- The increase in the amount of the mass flow of the solution (solution rich in NH_3) led to a decrease in the COP of the chiller, in a nearly linear way. This phenomenon occurs due to the dimensions of the heat exchangers (previously defined), i.e., the capacity of the heat exchanger was exceeded, which resulted in the COP of the chiller decreasing;
- The addition of the refrigerant heat exchanger to the prototype absorption refrigeration enabled the COP of the chiller to increase by approximately 3%.

ACKNOWLEDGEMENT

The first author is grateful to the program Science without borders - CNPq -Brazil, for the scholarship for the Post-doctoral study (PDE:203489/2014-4) and also to Professor Alberto Coronas for his support during the Post-doctoral study at the Rovira and Virgili University and also to the Staff of that university, especially the CREVER group. The authors thank FACEPE/CNPq for financial support for the research project APQ-0151-3.05/14 and also the CNPq for financial support for the research project - Universal 402323/2016-5.

NOMENCLATURE

A	Ratio enthalpy differences of the absorber, dimensionless
B	isotherm slope in Duhring Chart - "Coefficient of Duhring", dimensionless
C	Ratio enthalpy differences of the condenser, dimensionless
G	Ratio enthalpy differences of generator, dimensionless
Z	Intersept of the Duhring Equation, dimensionless
COP	Coefficient of Performance, dimensionless
$\dot{m}$	Mass flow rate [$kg.s^{-1}$]
h	Enthalpy [$kJ.kg^{-1}.K^{-1}$]
$\dot{Q}$	Heat Flow [kW]
S	Characteristic parameter - Proportion of the overall heat transfer coefficient of each component [$kW.K^{-1}$]
T	arithmetic mean internal temperature [°C]
t	arithmetic mean external temperature [°C]
UA	Heat transmission [$kW.K^{-1}$]
Δt	Temperature difference [K]
$\Delta\Delta t$	Total temperature difference or characteristic temperature function [K]
ΔTlm	Logarithmic mean temperature difference [°C]
NH_3	ammonia
$LiNO_3$	Lithium nitrate
X	Concentration of the solution [%]

Greek Symbols

α	Characteristic parameter - Distribution of the overall heat transfer coefficient inside the chiller [$kW.K^{-1}$]

Subscripts

A, a, C, c, G, g, E, e	Generator, absorber, evaporator, condenser
ec	Characteristic equation
gec	Generator characteristic equation
eec	Characteristic equation of the evaporator
diss, chi	Dissipated, chilled
max, loss	Maximum and loss heat
ref	Refrigerant
sol	Solution
thrust, lift	Thrust and lift temperature
strong, weak	Strong and weak solution
minE	Minimum evaporator
she, rhe	Solution heat exchanger and refrigerant heat exchanger
in, out	Inlet and outlet stream
X	Components
hot, cold	Hot and cold fluids
sat	Saturation state
exp	Data from the experimental test
Sim	Data obtained from the simulation
ch, ac	Chilled and cold water stream
e_exp_corr, g_exp_corr	Adjusted experimental correlation - Evaporator and generator

REFERENCES

Acuña, A., Velázquez, N., Cerezo, J. Energy analysis of a diffusion absorption cooling system using lithium nitrate, sodium thiocyanate and water as absorbent substances and ammonia as the refrigerant, Applied Thermal Engineering, 51, 1273-1281 (2013). https://doi.org/10.1016/j.applthermaleng.2012.10.046

Akrami, E., Nemati, A., Nami, H., Ranibar, F. Exergy and exergoeconomic assessment of hydrogen and cooling production from concentrated PVT equipped with PEM electrolyzer and LiBr-H_2O absorption chiller, International Journal of Hydrogen Energy, 43, 622-633 (2018). https://doi.org/10.1016/j.ijhydene.2017.11.007

Albers, J., Ziegler, F. Improved control strategies for solar assisted cooling systems with absorption chillers using a thermosyphon generator, In: Proceedings of the Int. Solar Air. Cond., October, Kloster Banz, Germany (2015).

Álvarez, M.E., Hernández, J.A., Bourois, M. Modelling the performance parameters of a horizontal falling film absorber with aqueous (lithium, potassium, sodium) nitrate solution using artificial neural networks, Energy, 102, 313-323 (2016). https://doi.org/10.1016/j.energy.2016.02.022

Amaris, C., Bourouis, M., Vallès, M., Salavera, D., Coronas, A. Thermophysical Properties and Heat and Mass Transfer of New Working Fluids in Plate Heat Exchangers for Absorption Refrigeration Systems, Heat Transfer Engineering, 36, 388-395 (2014). https://doi.org/10.1080/01457632.2014.923983

Azhar, M., Siddiqui, M.A. Energy and Exergy Analyses for Optimization of the Operating Temperatures in Double Effect Absorption Cycle, Energy Procedia, 109, 211-218 (2017). https://doi.org/10.1016/j.egypro.2017.03.043

Buonomano, A., Calise, F., Palombo, A. Solar heating and cooling systems by absorption and adsorption chillers driven by stationary and concentrating photovoltaic/thermal solar collectors: Modelling and simulation, Renewable and Sustainable Energy Reviews, 82, 1874-1908 (2018). https://doi.org/10.1016/j.rser.2017.10.059

Cai, D., He, G., Tian, Q., Bian, Y., Xiao, R., Zhang, A. First law analysis of a novel double effect air-cooled non-adiabatic ammonia/salt absorption refrigeration cycle, Energy Conversion and Management, 98, 1-14 (2015). https://doi.org/10.1016/j.enconman.2015.03.083

Cai, D., Jiang, J., He, G., Li, K., Niu, L., Xiao, R. Experimental evaluation on thermal performance of an air-cooled absorption refrigeration cycle with NH_3-$LiNO_3$ and NH_3-NaSCN refrigerant solutions. Energy Conversion and Management, 103, 32-43 (2016). https://doi.org/10.1016/j.enconman.2016.04.089

Cuenca, Y., Salavera, D., Vernet, A., Teja, A. S., Valles, M. Thermal conductivity of ammonia + lithium nitrate and ammonia + lithium nitrate + water solutions over a wide range of concentrations and temperatures, International Journal of Refrigeration, 38, 333-340 (2014). https://doi.org/10.1016/j.ijrefrig.2013.08.010

Chahartaghi, M., Golmohammadi, H., Shojaei, A.F. Performance analysis and optimization of new double effect lithium bromide-water absorption chiller with series and parallel flows, International Journal of Refrigeration, 97, 73-87 (2019). https://doi.org/10.1016/j.ijrefrig.2018.08.011

Domínguez-Inzunza, L. A., Hernández-Magallanes, J. A., Sandoval-Reyes, M., Rivera, W. Comparison of the performance of single-effect, half-effect, double-effect in series and inverse and triple-effect absorption cooling systems operating with the NH_3-$LiNO_3$ mixture, Applied Thermal Engineering, 66, 612-620 (2014). https://doi.org/10.1016/j.applthermaleng.2014.02.061

Farshi, L. G., Infante-Ferreira, C. A., Mahmoudi, S. M. S. First and second law analysis of ammonia/salt absorption refrigeration systems, International Journal of Refrigeration, 40, 111-121 (2014). https://doi.org/10.1016/j.ijrefrig.2013.11.006

Guido, W.H., Laner, W., Petersen, S., Ziegler, F. Performance of absorption chillers in field tests, Applied Thermal Engineering, 134, 353-359 (2018). https://doi.org/10.1016/j.applthermaleng.2018.02.013

Hernández-Magallanes, J. A., Domínguez-Inzunza, L. A., Gutiérrez-Urueta, G., Soto, P. Jiménez, C., Rivera, W. Experimental assessment of an absorption cooling system operating with the ammonia/lithium nitrate mixture, Energy 78, 685-692 (2014). https://doi.org/10.1016/j.energy.2014.10.058

Herold K. E., Radermacher R., Klein S. A. Absorption Chillers and Heat Pumps. 2nd Edition, CRC, Press LLC, USA (2016). https://doi.org/10.1201/b19625

Jiang, J., Liu, Y., He, G., Liu, Y., Cai, D., Liang, X. Experimental investigations and an updated correlation of flow boiling heat transfer coefficients for ammonia/lithium nitrate mixture in horizontal tubes, International Journal of Heat and Mass Transfer, 112, 224-235 (2017). https://doi.org/10.1016/j.ijheatmasstransfer.2017.04.135

Jiménez, C., Rivera, W. Experimental assessment of an absorption cooling system operating with the ammonia/lithium nitrate mixture, Energy, 78, 685-692 (2014). https://doi.org/10.1016/j.energy.2014.10.058

Kohlenbach, P., Ziegler, F. A dynamic simulation model for transient absorption chiller performance. Part II: Numerical results and experimental verification, International Journal of Refrigeration, 31, 226-233 (2008). https://doi.org/10.1016/j.ijrefrig.2007.06.010

Libotean, S., Martin, A., Salavera, D., Valles, M., Esteve, X., Coronas, A. Densities, Viscosities, and Heat Capacities of Ammonia + Lithium Nitrate and Ammonia + Lithium Nitrate + Water Solutions between (293.15 and 353.15) K, Journal of Chemical and Engineering Data, 53, 2383-2388 (2008). https://doi.org/10.1021/je8003035

Libotean, S., Salavera, D., Valles, M., Esteve, X., Coronas, A. Vapor-Liquid Equilibrium of Ammonia + Lithium Nitrate + Water and Ammonia + Lithium Nitrate Solutions from (293.15 to 353.15) K, Journal of Chemical and Engineering Data, 52, 1050-1055 (2007). https://doi.org/10.1021/je7000045

Maryami, R., Dehghan, A.A. An exergy based comparative study between LiBr/water absorption refrigeration systems from half effect to triple effect, Applied Thermal Engineering, 124, 103-123 (2017). https://doi.org/10.1016/j.applthermaleng.2017.05.174

Moreno-Quintanar, G., Rivera, W., Best, R. Comparison of the experimental evaluation of a solar intermittent refrigeration system for ice production operating with the mixtures $NH_3/LiNO_3$ and $NH_3/LiNO_3/H_2O$. Renewable Energy, 38, 62-68 (2012). https://doi.org/10.1016/j.renene.2011.07.009

Myat, A., Thu, K., Kim, Y. D., Chakraborty, A., Chun, W. G., Choon, K. N. A second law analysis and entropy generation minimization of an absorption chiller, Applied Thermal Engineering, 31, 2405 - 2413 (2011). https://doi.org/10.1016/j.applthermaleng.2011.04.004

Ochoa, A.A.V., Dutra, J.C.C., Henríquez, J.R.G., Rohatgi, J. Energetic and exergetic study of a 10RT absorption chiller integrated into a microgeneration system, Energy Conversion and Management, 88, 545-553 (2014). https://doi.org/10.1016/j.enconman.2014.08.064

Ochoa, A.A.V., Dutra, J.C.C., Henríquez, J.R.G., Santos, C.A.C. dos. Dynamic study of a single effect absorption chiller using the pair LiBr/H2O, Energy Conversion and Management, 108, 30-42 (2016). https://doi.org/10.1016/j.enconman.2015.11.009

Ochoa, A.A.V., Dutra, J.C.C., Henríquez, J.R.G., Santos, C.A.C. dos, Rohatgi, J. The influence of the overall heat transfer coefficients in the dynamic behavior of a single effect absorption chiller using the pair $LiBr/H_2O$, Energy Conversion and Management, 136, 270-282 (2017). https://doi.org/10.1016/j.enconman.2017.01.020

Ochoa, A.A.V., Costa, J.A.P. da, Franco, S.S. Implementation of the Characteristic Equation Method applied to an Absorption Chiller $LiBr/H_2O$ of Commercial type, CIENTEC, 9, 24-38 (2017).

Puig, A. M., López, V. J., Bruno, J. C. Coronas, A. Analysis and parameter identification for characteristic equations of single - and Double effect absorption chillers by means of multivariable regression, International Journal of Refrigeration, 33, 70-78 (2010). https://doi.org/10.1016/j.ijrefrig.2009.08.005

Sabbagh, A.A., Gómez, J.M., Optimal control of single stage LiBr/water absorption chiller, International Journal of Refrigeration, 92, 299-311 (2018). https://doi.org/10.1016/j.ijrefrig.2018.05.007

Tillner-Roth, R., Harms-Watzenberg, F., Baehr, H.D. A new fundamental equation for ammonia. DKV-Tagungsbericht, 20, 167-181 (1993). (*in German*).

Ventas, R., Lecuona, A., Rodriguez-Hidalgo, M.C. Performance analysis of an absorption double-effect cycle for power and cold generation using ammonia/lithium nitrate, Applied Thermal Engineering, 115, 256-266 (2017). https://doi.org/10.1016/j.applthermaleng.2016.12.102

Ventas, R., Lecuona, A., Vereda, C., Legrand, M. Two-stage double-effect ammonia/lithium nitrate absorption cycle, Applied Thermal Engineering, 94, 228-237 (2017). https://doi.org/10.1016/j.applthermaleng.2015.10.144

Wang, J., Li, X., Wang, B., Wu, W., Song, P., Shi, W. Performance Comparison between an Absorption-compression Hybrid Refrigeration System and a Double-effect Absorption Refrigeration System, Energy Procedia, 205, 241-247 (2017). https://doi.org/10.1016/j.proeng.2017.09.959

Zamora, M. Optimización industrial y estrategia de control de una enfriadora de absorción de amoniaco/nitrato de litio con disipación por aire. Ph.D thesis. Universitat Rovira i Virgili, Spain (2012).

Zamora, M., Bourouis, M., Coronas, A., Vallès, M. Part-load characteristics of a new ammonia/lithium nitrate absorption chiller, International Journal of Refrigeration, 56, 43-51 (2015). https://doi.org/10.1016/j.ijrefrig.2014.11.005

Zamora, M., Bourouis, M., Coronas, A., Vallès, M. Pre-industrial development and experimental characterization of new air-cooled and water-cooled ammonia/lithium nitrate absorption chillers, International Journal of Refrigeration, 45, 189-197 (2014). https://doi.org/10.1016/j.ijrefrig.2014.06.005

Zinet, M., Rulliere, R., Haberschill, P. A numerical model for the dynamic simulation of a recirculation single-effect absorption chiller, Energy Conversion and Management, 62, 51-63 (2012). https://doi.org/10.1016/j.enconman.2012.04.007